Archives of Razi Institute, Vol. 76, No. 4 (2021) 795-808

DOI: 10.22092/ari.2021.355997.1758

Original Article

Determination of Ferrous Oxide Nanoparticles Minimum Inhibitory Concentration against Local Virulent Bacterial Isolates

Al-Rawi, M[1], Al-Mudallal, N. H. A. L[1 *], Taha, A. A[2]

1. Department of Medical Microbiology, College of Medicine, Al-Iraqia University, Baghdad, Iraq
2. Department of Applied Science, Division of Biotechnology, University of Technology, Baghdad, Iraq

Received 6 September 2021; Accepted 21 September 2021
Corresponding Author: nada_mudallal@aliraqia.edu.iq

Abstract

The improvement of multi-resistance properties of the bacterial pathogen has recently been discussed as an emerging issue. In this regard, iron oxide nanoparticles have attracted the researchers' attention due to their wide application in the realm of medicine. Iron oxide nanoparticles have a high specific surface area that enables them to interact with the bacterial surface structure and has considerable antibacterial activity. The current study aimed to synthesize a novel antimicrobial agent from iron oxide nanoparticles and determine its minimum inhibitory concentration (MIC) on different gram-positive and negative variant bacterial strains isolated and characterized from the infected urinary tract of Iraqi elderly patients. This study was conducted from September 2020 to December 2020 on 75 urine samples collected from the infected urinary tract of elderly patients in the ages range of 60-75 years admitted to Al-Yarmouk Medical Hospital, Baghdad, Iraq. Isolation of bacterial isolates was carried out using differential and selective media. Afterward, they were characterized and confirmed using different biochemical tests and VITEK 2 system, respectively. Magnetic nanoparticles were fabricated by co-precipitation of ferric ions (Fe^{3+}) and ferrous ions (Fe^{2+}) in presence of ammonium hydroxide solution (25%). The characterization of synthesized nanoparticles was performed subsequently using UV-VIS spectroscopy analysis, Scanning Electron Microscope (SEM), Fourier transform infrared spectroscopy analysis, X-ray Diffraction analysis (XRD), and Energy-dispersive X-ray spectrum (EDX). The MIC of synthesized sonicated Fe_3O_4NP against different bacterial strains was determined using the broth culture dilution method through making serial dilutions of 50, 100, 200, 400, 500, 600, 800, 900 µg/ml from a 5mg/ml nanoparticle stock solution. Afterward, the lowest concentration of nanoparticles required to arrest the growth of bacteria was determined through the colony-forming unit of each treated bacteria on brain heart infusion agar. In total, 17bacterial isolates were identified from the infected urinary tract, five bacterial isolates (*E. coli, Pseudomanas aeruginosa, Staphylococcus aureus, Enterococcus faecalis, and Micrococcus luteus*). In addition, two *Proteus mirabilis* strains were identified separately and were tested against synthesized Fe_3O_4NP to determine the MIC. The novel synthesized antibacterial agent showed excellent bioactivity, compared with controls (consisting of bacterial suspension without ferrous oxide nanoparticles), and the synthesized antibacterial agent was considered significantly active against all the bacterial strains at a p-value less than 0.05. The Fe_3O_4NP were active against gram-negative more than gram-positive bacteria. The MIC of synthesized and characterized Fe_3O_4NPwas applied on seven gram-positive and negative bacterial isolates using bacteria- Fe_3O_4NP complex. Significant effects were observed on all strains, compared with controls, and this complex could significantly inhibit gram-negative more than gram-positive bacteria.

Keywords: Iron Oxide NPs, Bacterial Strains, UTI Elderly Patients, Minimum inhibitory concentration

1. Introduction

Urinary tract infections (UTIs) are one of the most infectious diseases with an extensive financial burden on society. UTI is a bacterial infection of the urinary bladder, kidney, or collecting system. This condition may be either acute or chronic and may affect any part of the upper or lower urinary system (1). UTI is common in the Iraqi population and accounts for 23% of all infections (2). UTI is one of the most commonly diagnosed infections in older adults. It is the most frequently diagnosed infection in long-term care residents, accounting for over a third of all nursing cases home-associated infections (3). It is second only to respiratory infections in hospitalized patients and community-dwelling adults over the age of 65 years (4). UTI is one of the most important recurrent diseases worldwide, especially in the Middle East countries and the second most common condition in both males and females with the rate of 1/2, respectively (5, 6).

UTI is often caused by Extended-Spectrum β-Lactamase ESBL-producing gram-negative bacteria, such as *Escherichia coli* (*E. coli*), *Klebsiella pneumonia* (*K. pneumonia*), and *Pseudomonas aeruginosa* (*P. aeruginosa*) (7). Almost all these pathogens, such as *Proteus mirabilis* and *Providencia* are multi-drug resistant and cause clinical problems with limited therapeutic options (5, 8). Gram-positive organisms, such as methicillin-resistant *Staphylococcus aureus* and *Enterococcus* are less common overall; however, these are started to be considered with increasing interest in the healthcare settings and among adults with chronic indwelling catheters (9).

In the last two decades, the metal oxides of the transition metals (TM) have been used in a very wide range of applications, such as sensors, adsorbents, catalysts, conductors, magnetic, and super conductors due to their unique and exceptional physic-chemical characteristics that enable them to be used in electrochemistry, environmental science, and biology (10, 11). Iron oxide is one of the TM oxides with special morphology and other properties in its nanoscale structure that enable it to have variant applications. This element can act as an antimicrobial agent in treating and preventing infectious diseases in animal and human beings, which enables the researchers to adopt it as a new class of materials in nanobiotechnology, biomedical, and pharmaceutical industries (12).

The high specificity of iron nanoparticles produced via certain biosynthesis methods lies in their interaction with the surface of the bacterial structures, other than their small size, that enable them to attract bacteria cells at the molecular level (13).

Cohen (14) showed that the use of antimicrobial agents plays an important role in reducing the effect of infectious diseases and decreasing the percentage of death. In addition, many studies and researches indicated that NPs can be used as antibacterial agents and showed that their impacts may vary depending on their structure. Therefore, these have different influences on the pathogenic bacteria by limiting their activity and preventing them from developing diseases (15). However, Masadeh and Karasneh Masadeh, Karasneh (16) suggested that using metal oxide NP scan be applied as an antibacterial agent. Accordingly, iron oxide (Fe_2O_3) and cerium oxide (CeO_2) nanoparticles can be used as antibacterial agents against gram-negative and gram-positive bacteria. Moreover, the obtained results showed that these nanoparticles can interfere with the action of antibiotics.

Das, Diyali (10) found that FeNPs caused damage, destructed the mitochondria membrane of *Staphylococcus aureus*, and were clinically approved as an antibacterial agent.

The current study aimed to isolate and identify gram-positive and gram-negative bacteria from urine samples of elderly Iraqi patients with UTI. Moreover, the MIC of the prepared iron oxide NPs was determined against the growth of these isolates.

2. Material and Methods

2.1. Sample Collection

Urine samples (n=75) were collected from UTI elderly patients in the age range of 60-75 years

admitted to Al-Yarmouk Medical Hospital, Baghdad, Iraq, from September 2020 to December 2020. Midstream and catheterized urine samples were put in sterile wide-mouthed containers and immediately transported to the laboratory for further investigation.

2.2. Isolation and Identification of Bacteria

Samples were immediately cultured on the surface of MacConkey agar media, which were used to differentiate gram-negative from gram-positive bacteria, as well as on blood agar media for isolation of gram-positive bacteria. Cultures were incubated aerobically at 37ºC for 18-24 h. Macroscopic features of bacterial colonies were described by shape, color, arrangement, and the height of colonies on these media. Moreover, the microscopic features of bacterial cells were observed after they were stained with gram stain under a light microscope.

2.3. Biochemical Tests

All tests were conducted according to the procedure explained in the study conducted by M Tille (17). Different biochemical tests (e.g., urea, oxidase, catalase, indole, citrate utilization, Kligler's Iron Agar, hemolysis on blood agar, coagulase, bile esculin agar, and deoxyribonuclease tests) were performed to identify different gram-positive and negative bacteria. The identified bacteria were confirmed using VITEK 2 system. *Proteus mirabilis* isolate was isolated and identified separately from the total bacterial isolates in Al-Yermook Teaching Hospital Lab, Baghdad, Iraq. Moreover, a standard strain of *Proteus mirabilis* was isolated from UTI patients and identified by molecular technique. Furthermore, phylogenetic analysis was conducted based on the method described by Al-Mudallal N. H. A. L., Khudair A. M. (18).

2.4. Chemical Synthesis of Fe_3O_4NP

The magnetic nanoparticles were fabricated using co-precipitation of ferric ions (Fe^{3+}) and ferrous ions (Fe^{2+}) in the presence of ammonium hydroxide solution (25%), according to the method described by Alzahrani (19). This was performed by dissolving 4.58 g of $FeCl_2.4H_2O$ and 8.93 g of $FeCl_3.6H_2O$ in 80 mL distilled water. The mixture was then heated to 80°C with vigorous stirring (1,100 rpm). Subsequently, 10 mL of ammonium hydroxide (NH4OH) solution was added to the mixture. The reaction was allowed to continue for 30 min to ensure the complete growth of nanoparticle crystals under the same conditions. The resulting suspension was then cooled down to room temperature and washed with distilled water several times. Eventually, the magnetic nanoparticles were isolated using an external magnetic field, dried in a hot air oven (Memmert, Germany) at 50 °C, and then weighted by digital balance.

2.5. Characterization of Fe_3O_4NP

2.5.1. UV-VIS Spectroscopy Analysis

The UV analysis was carried out by scanning the prepared solution of Fe_3O_4NP using a UV-Vis spectrophotometer in the range 190-900 nm (20).

2.5.2. Scanning Electron Microscopic (SEM)

The molecule size and morphology of Fe_3O_4NPs and the SEM analysis were determined at the Materials Research Department of the Ministry of Science and Technology, Baghdad, Iraq. Thin sample films were prepared on a cover slide grid by dropping a very small amount of the sample on the cover slide, which was then dried at room temperature (21).

2.5.3. Fourier Transform Infrared (FTIR) Spectroscopy Analysis

The FTIR analysis was performed on chemical bonds of the prepared Fe_3O_4NPs through scanning at wavelength ranges 400-4000 cm^{-1}. The FTIR assay was conducted in the Applied Chemistry Division, Department of Applied Sciences, University of Technology, Baghdad, Iraq.

2.5.4. X-ray Diffraction (XRD) Analysis

The XRD assay was performed in Central Service Laboratory, College of Pure Science Education, IbnAl-Haytham University, Baghdad, Iraq. The XRD measurements were determined after sedimentation of the sample on a glass slide in a $1cm^2$ area. The operation was conducted at a voltage of 40 kV and a

current of 30 mA with Cu radiation at a scan range of 5.0000-80.0000 degrees (20).

2.5.5. Energy-Dispersive X-ray Spectrum (EDX)

The EDX is a qualitative and quantitative X-ray micro-analytical technique that provides information on the chemical composition of a sample for elements with atomic number Z>3. The EDX analysis was performed at the Materials Research Department, Ministry of Science and Technology, Baghdad, Iraq (22).

2.6. Determination of Minimum Inhibitory Concentrations of Fe_3O_4NPs

2.6.1. Preparation of Bacterial Isolates

The MIC of Iron oxide NPs was determined against gram-positive and negative bacteria. Briefly, bacterial cell growth suspension after overnight incubation at 37ºC in 5ml brain heart infusion broth was adjusted to 0.5 McFarland turbidity (equivalent to 1.5×10^8Colony-forming unit [CFU]). Afterwards,0.1 ml of bacterial cell growth suspension was added to 9.9 ml brain heart infusion broth to reach the concentration of 1.5 x 10^6 CFU representing bacterial growth stock culture.

2.6.2. Preparation of Fe_3O_4NP

The Fe_3O_4NP0.001 gram was dissolved in 2 ml of dimethyl sulfoxide to get a concentration of 5mg/ml. The solution was then placed in an ice bath and exposed to ultrasound waves for 5 min using a sonicator until it became colloidal.

2.6.3. Minimum Inhibitory Concentration of Fe_3O_4NPs

The MIC of synthesized sonicated Fe_3O_4NPagainst different bacterial strains were determined using the tube dilution method in culture broth via making serial dilutions (50, 100, 200, 400, 500, 600, 800, 900 µg/ml) from a 5 mg/ml stock of nanoparticles with bacterial growth stock culture incubated for 24 h at 37ºC.The MIC was then determined through the observation of the lowest concentration of nanoparticles required to arrest the growth of bacteria after determining the CFU of each treated bacteria on brain heart infusion agar, compared with the untreated control that was prepared with the same bacterial stock using distilled water instead of iron oxide colloidal solution.

2.7. Statistical Analysis

The statistical analysis was performed using SPSS software (Version 27). Data were presented in simple measures of frequency, percentage, mean, standard deviation, and range (minimum-maximum values). The significance of difference was tested using Student's t-test for the difference between two independent means. The significance of the difference between different bacterial species was used to test Least significant difference. Ap-value equal to or less than 0.05was considered statistically significant (23, 24).

3. Results

3.1. Isolation and Identification of Bacteria

The data in figure 1 represent the growth of isolated bacteria on the surface of MaCconkey agar and blood agar media. Out of75 urine samples, no growth was observed in 58samples and the quantitative count of bacteria was less than10^5 CFU in one urine specimen. Only 17bacterial isolates were isolated on these media and they were examined in terms of colonial morphology, colors, arrangements, and heights, as well as their ability or inability to ferment lactose. Microscopic examination of these isolates performed after their viability was confirmed by gram staining, and they were differentiated to either gram-positive cocci or gram-negative rods.

3.2. Biochemical Tests

The obtained results are presented in tables 1 and 2 and figures 2 and 3.

According to the biochemical tests and VITEK 2 system conformational reports of all 17bacterial isolates, 5 bacterial isolates were chosen to undergo MIC testing (*E. coli*, *Pseudomanas aeruginosa*, *Staphylococcus aureus*, *Enterococcus faecalis*, and *Micrococcus luteus*). Two *Proteus mirabilis* strains were identified separately as well.

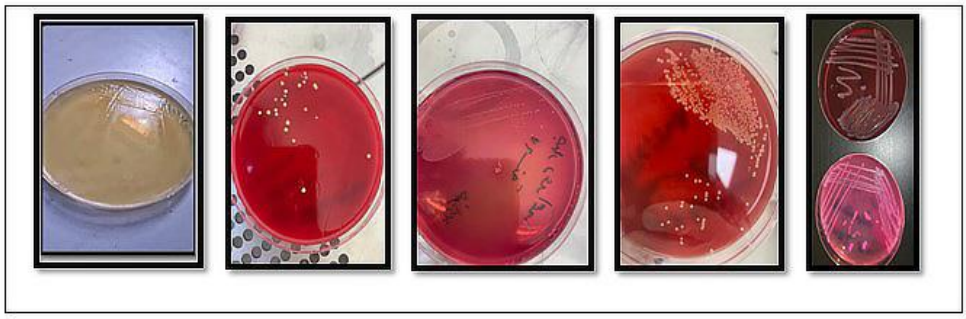

Figure 1. The growth of isolated bacteria on the surface of MaCconkey agar and Blood agar

Table 1. Biochemical tests of gram-negative bacterial isolates

Bacterial isolates	Gramstain	Citrate test	Lactose fermentation	Indol test (Peptone water)	Kigler iron agar test	Urease test	Oxidase test	Catalase
E .coili	-	-	+	+	A\A+ GAS	-	-	+
P.aerugenosa	-	+	-	-	K\K_	-	+	+

Table 2. Biochemical tests of gram-positive bacterial isolates

Gram positivebacteria isolate	Gram stain	Citrate test	Lactose Fermentation	Oxidase	Catalase	Coagulase	Bile Esculin test	DNAase
Enterococcus feacalis	+	_	+	_	_	_	+	_
Staphylococcus aureus	+	+	No growth	_	+	+	_	+
Micrococcus luteus	+	+	No growth	+	+	+	_	_

Figure 2. Some biochemical tests used in the identification of bacterial isolates (Esculin, Catalase, Citrate, Kligler iron, and Indole tests)

3.3. Chemical Synthesis of Fe_3O_4NP

The weight of dried magnetic Fe_3O_4NPs was determined to be 14.5 grams, according to the procedure mentioned in 2.4 (Figure 3).

3.4. Characterization of Fe_3O_4NPs

The UV-Visible spectra of Fe_3O_4NPs were determined (Figure 4). The technique has been used to verify the formation of iron oxide nanoparticles. The peak of iron oxide NPs was observed at 274 nm.

Moreover, FTIR spectroscopy is used to determine the functional groups in the prepared solid materials as shown in figure 5.

On the other hand, XRD is used to determine the crystal structure and particle size of prepared crystalline nanomaterials (Figure 6).

The EDX is used as a diagnostic tool to identify the elementary components of the chemical composition of the prepared samples. The EDX spectrum of iron oxide NPs is presented in figure 7. The peaks of iron and oxygen elements were observed, indicating the formation of iron oxide compounds. The iron, oxygen, and carbon ratio were determined to be 69.4 wt %, 14.9 wt %, and 8.8 wt %, respectively.

Furthermore, the SEM was used to provide information about the surface morphology and particle size of the prepared samples (Figure 8).

3.5. Determination of MIC of Fe_3O_4NPs

As indicated by the data presented in table 3 and figure 9, the Fe_3O_4NP have an antibacterial effect against all bacterial isolates, compared with controls. Moreover, the lowest MIC of synthesized Fe_3O_4NP was determined to be 550 µg/ml.

The level of gram-negative bacteria was $148.0\pm60.5x10^3$cfu after treatment with Fe_3O_4NP, compared with controls ($16.6\pm12.23x10^6$cfu). The P-value between gram-positive and negative bacteria was recorded to be 0.218, compared with controls (0.0001*).

Figure 3. Dried magnetic nanoparticles isolated using an external magnetic field

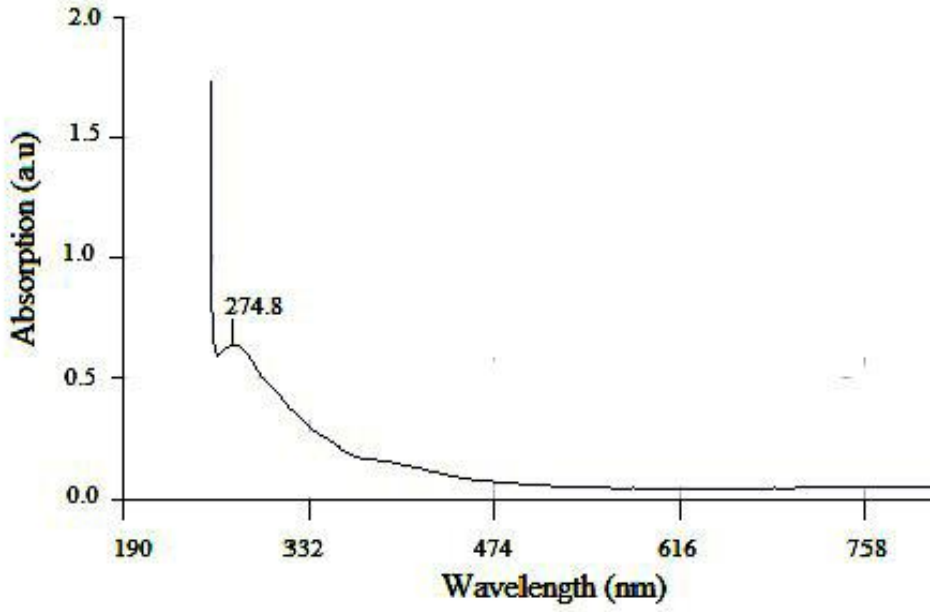

Figure 4. UV/V is spectra of iron oxide Fe_3O_4NPs

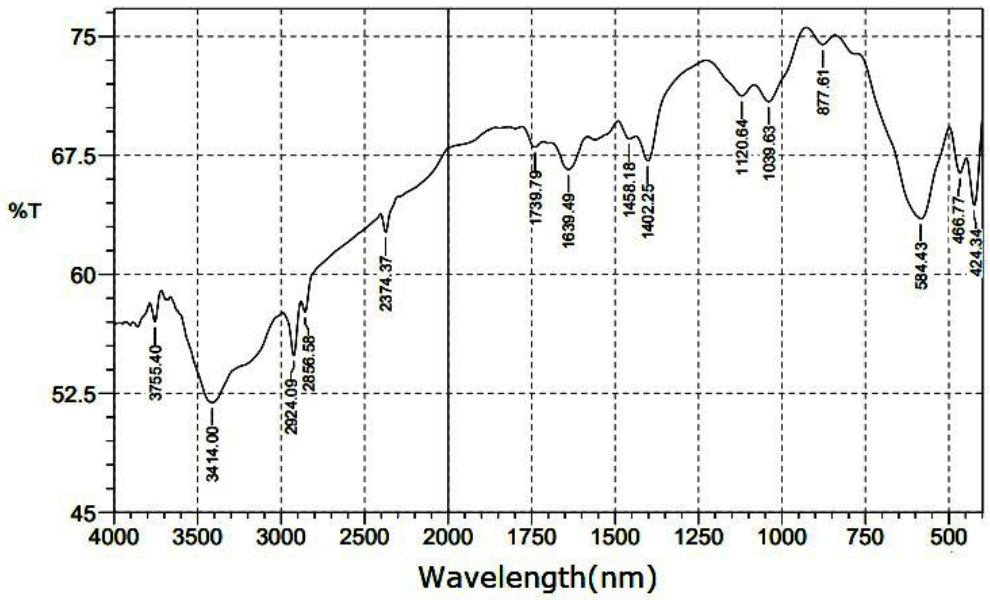

Figure 5. FTIR of iron oxide NPs

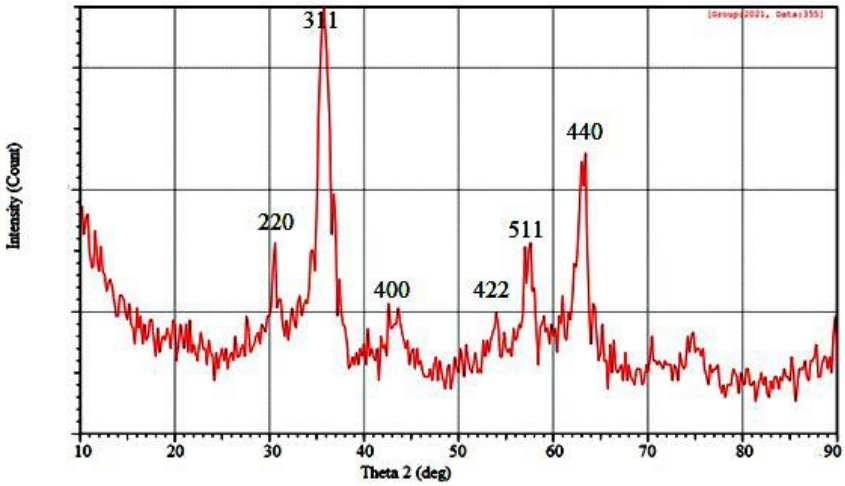

Figure 6. XRD pattern of iron oxide NPs

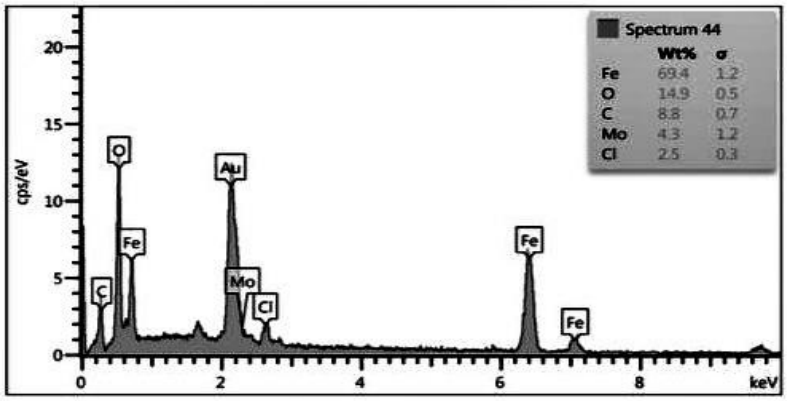

Figure 7. EDX to iron oxide NPs

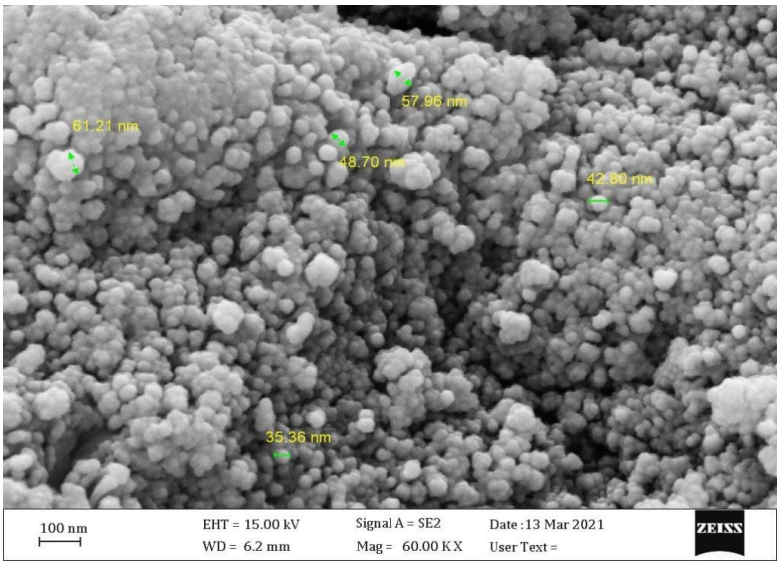

Figure 8. SEM of iron oxide NPs

Table 3. The minimal inhibitory concentration of Fe_3O_4NP against bacterial isolates, compared with controls

Bacterial Isolates	(MIC) of Ferrous oxide nanoparticles (µg/ml)	Ferrous oxide NP exposed (CFU x 10^3)	Not treated (Control x 10^6)	P-value
Enterococcus fecalis	700	150±16.7(135-168)	80±14.6 (66-95)	0.011*
Pseudomonasaerginosa	550	52±3.0 (49-55)	35±4.58 (30-39)	0.006*
Micrococcus	850	160±8.5 (152-169)	75±10.8 (63-84)	0.007*
Staph. aureus	800	30±6.6 (23-36)	66±6.56 (59-72)	0.003*
Proteus mirabilis (1)	850	200±14.8(183-210)	4.7±0.58 (4-5)	0.005*
Proteus mirabilis (2) *(standard)*	850	180±9.8 (172-191)	9.7±0.58 (9-10)	0.001*
E coli	850	160±12.3(151-174)	17±2.65 (14-19)	0.008*

*Significant difference between two independent means using Students' t-test at 0.05 level.
-Data were presented as Mean±SD (Range)
Cfu (colony forming unit)

Table 4. Antibacterial activity of Iron oxide nanoparticles against gram-positive and gram-negative bacteria

Bacterial Isolates	Ferrous oxide NP exposed (CFU x 10^3)	Not treated (Control x 10^6)	P-value
Gram +ve	113.3±63.4 (23-469)	73.7±11.4 (59-95)	0.0001*
Gram –ve	148.0±60.5 (49-210)	16.6±12.23 (4-39)	0.0001*
P-value	0.218	0.0001*	

*Significant difference between two independent means using Students-test at 0.05 level.
-Data were presented as Mean±SD (Range)

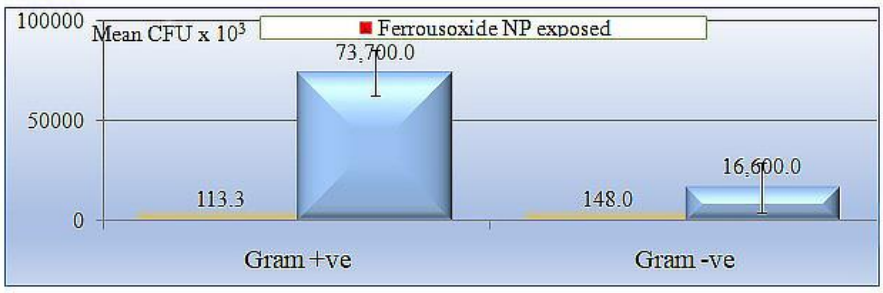

Figure 9. Antibacterial activity of ferrous oxide nanoparticles against gram-positive and negative bacterial isolates determined by statistical analysis, compared with controls

4. Discussion

A symptomatic UTI is generally defined by the presence of urinary tract-specific symptoms in the setting of significant bacteriuria with a quantitative count of $\geq 10^5$ CFU/ml in one urine specimen. Asymptomatic bacteriuria (ASB) is defined as the presence of bacteria in the urine, without clinical signs or symptoms suggestive of a UTI (25, 26). UTI and ASB are highly prevalent in older adults; however, the risk factors for developing symptomatic UTI in the aging population are different from those in a younger population. Age-associated changes in immune function, corticosterol and indwelling urethral catheters, exposure to nosocomial pathogens, and increasing number of comorbidities put the elderly at an increased risk for developing infection (27).The high incidence of urine samples with no growth (n=58) from the total 75 samples can be explained by the possibility that patients may have been given antimicrobial drugs that inhibit the growth of bacteria or to the presence of *candida spp*. or anaerobic bacteria that grow on another types of media and specific incubation environmental conditions. In addition, the quantitative count of bacteria was less than$\geq 10^5$CFU in one urine specimen. Both gram positive and negative bacteria isolated in this study included *E. coli, Staphylococcus aureus, Enterococcus faecalis, Pseudo Manas Aeruginosa, and Micrococcus luteus* in descending order of prevalence. The fact that *Staphylococcus spp.*is a normal flora of the perianal and vaginal region may account for the high prevalence of *Staphylococcus spp*. Abdulrahman (28) showed that the distribution of microbial species caused UTIs in the Duhok, Iraq,in2014 and 2015, and the common uropathogens in this study included *E. coli* (52%), followed by *S. aureus*(11%).While the results of another study conducted in the city of Duhok, Iraq, revealed that *Enterococcus faecalis* is the second most common uropathogen in this region(29).

Recently, iron NPs have attracted much attention due to their unique properties, including super paramagnetism, surface-to-volume ratio, greater surface area, and easy separation methodology. Iron oxide magnetic NPs with appropriate surface chemistry are prepared by various methods, including wet chemical, dry processes, or microbiological techniques (30, 31). The investigation of iron and iron oxide NPs in biological and material sciences is booming in recent years due to their various chemical and physical properties. They exhibit multiple potential applications in magnetic fluids, magnetic micro-devices, MRI, magnetic hyperthermia, water purification, and drug delivery (32, 33). Significant size-dependent structural and optical properties of colloidal iron and iron oxide NPs correspond to electrical structure and quantum size effects of NPs. Moreover, the respective synthesis method of iron oxide NPs can affect their size and crystal structure as well. The most effective, cheap, and simple technique to obtain magnetic particles is the precipitation technique for obtaining iron oxide particles (34).

In this study, magnetic nanoparticles were fabricated by coprecipitation of Fe^{2+} and Fe^{3+} salts from an aqueous solution by the addition of ammonium hydroxide solution as a base. The fabricated magnetic nanoparticles have super magnetic properties which make them susceptible to magnetic fields and lead to their easy separation from the solution (19).

Comprehensive surface characterization techniques, such as surface morphology, chemical composition, and spatial distribution of the functional groups are used for a better understanding of surface properties of Fe_3O_4NP (35). Fundamental techniques employed to investigate magnetic NPs include X-ray diffraction analysis, FTIR, TEM, SEM, atomic force microscopy, X-ray photoelectron spectroscopy, vibrating sample magnetometry, and thermal gravimetric analysis (36).

In this study, FTIR spectroscopy is used to determine the functional groups in the prepared solid materials as presented in Figure 6. The transmission FTIR spectra of iron oxide NPs is in a range of 400-4000 cm^{-1}. The appearance of a weak absorption peak at 3414 $cm^{-1}$is due to the stretching vibration of the hydroxyl groups, indicating the absorption of water molecules on the surface of the prepared sample. However, the apparent

absorption peak at 1639.49 cm^{-1} is due to the O-H bending vibration. Eventually, the strong absorption peak at 877.61 cm^{-1} is due to the Fe-O bonds vibration. On the other hand, XRD is used to determine the crystal structure and particle size of prepared crystalline nanomaterials (Figure 7). The XRD pattern of iron oxide NPs exhibited the diffraction peaks of 2θ=30.77°, 36.42°, 43.48°, 54.53°, 56.78°, and 62.28°, corresponding to the planes of 220, 311, 400, 422, 511, and 440, respectively. The nonappearance of other peaks in the spectrum indicates the high purity of the iron oxide NPs (37).

Furthermore, SEM was used to provide information about surface morphology and particle size of the prepared samples as shown in Figure 9. The microscopic images revealed the formation of spherical nanoparticles of different sizes and distributions. The average particle size of iron oxide NPs is from35.36 to 61.21 nm. The increase in the rate of particle agglomeration was due to the electrostatic interaction between the layers of nanoparticles.

Moreover, great attention has been paid to iron oxide nanoparticles for their use in designing therapeutics, targeted drug delivery, and other biomedical applications due to such features as large surface area, small size, lower nanotoxicity, appealing magnetic properties, and harmlessness for the environment (38, 39). The antibacterial activity of the synthesized Fe_3O_4NP was tested against seven bacterial variant isolates for determination of MIC according to the CFU counting results that had been calculated for all bacteria on the surface of brain heart infusion agar. The results were then compared with CFU counting results of the untreated control for each bacterial isolate. The data presented in Tables 3-4 indicate that Fe_3O_4NP have antibacterial activity against all the bacterial isolates. Based on the p-values, standard strains of *Proteus mirabilis* were the most affected bacteria at MIC 850 µg/ml (P=0.0001) (2), while *Enterococcus faecalis* represented the least affected bacterial isolate by the Fe_3O_4NP (P=0.011) at MIC of 700 µg/ml. The lowest MIC for synthesized Fe_3O_4NP (550µg/ml) was determined against *Pseudomonas aeruginosa* with 52±3.0 $x10^3$CFU, compared with untreated control (35±4.58 $x10^6$CFU). However, the highest MIC (850 µg/ml) was determined against *Micrococcus luteus*, *Proteus mirabilis* (1), *Proteus mirabilis* (2) standard, and *E. coli* with CFU of 160±8.5 $x10^3$, 200±14.8 $x10^3$, 180±9.8 $x10^3$and 160±12.3 $x10^3$, respectively, compared with CFU of untreated control at 75±10.8 $x10^6$, 4.7±0.58 $x10^6$, 9.7±0.58 $x10^{6,}$ and 17±2.65$x10^6$, respectively. According to the results, MIC of Fe_3O_4NP represented a better inhibitory effect against *P. aeroginosa*, while according to the CFU P-values, these nanoparticles represented a better antibacterial effect on Proteus mirabilis (2) standard strains. In addition, Fe_3O_4NP exhibited significant antibacterial efficacy against gram-negative bacteria, compared with gram-positive bacteria, according to the CFU of gram-negative and positive bacteria in comparison with untreated control.

Das, Diyali (10) determined the bactericidal activity of iron oxide nanoparticles against *Staphylococcus aureus*, *Proteus vulgaris*, and *Psedomonas aeruginosa*, as the nanoparticles that exhibit bactericidal activity against all bacterial isolates and the most affected bacteria was *Staphylococcus aureus* with MIC of 12.5 µg/mL. It was observed that the IONPs displayed a little less activity compared to the streptomycin as a standard medication, indicating that it can be used as antibacterial drug due to increased resistance to existing antibiotics of various microorganisms. Madhu, Jaianand (40) estimated the antibacterial properties of IONP against gram positive and negative bacteria (41) and concluded that this NP affected the growth of both types of bacteria; however, it could inhibit gram positive more than gram negative bacterial strains. Prodan, Iconaru (41) determined the antimicrobial activity of the iron oxide NPs on strains belonging to common bacterial pathogens, the Gram-negative *P. aeruginosa* and *E. coli*, Gram-positive *E. faecalis* and *B. subtilis*, and a yeast strain of *C. krusei* with MIC

experiment for the sensitive bacterial strains. A bactericidal effect has been observed at low concentrations of iron oxide NPs (i.e., from 0.039 to 0.01mg/mL) against *E. faecalis* and *P. aeruginosa* and from 0.02 to 0.01 against *E. coli*. The IO-NPs exhibited no inhibitory effect on *C. krusei* and *B. subtilis* growth, irrespective of the tested concentration.

Metal oxide nanoparticles, including magnetite, proved to have inherent antimicrobial properties which occur or are enhanced when the materials are in then a 0 meter size and in relation to the surface area (42). Since nanoparticles can be smaller in size than bacterial pores, they have a unique ability to cross the cell membrane, disrupt its function, or interfere with nucleic acid or protein synthesis (43). The increment nature of reactive oxygen species (ROS) observed in all aerobic bacteria upon treatment of IONPs, the bacterial cell may cause the damage of iron-sulfur clusters as well as IONPs, thereby release ferrous ion. The Fe2þ ions can then react with H_2O_2 through the Fenton reaction to produce hydroxyl radical which can destroy bacteria's DNA, lipid, and proteins (44). This phenomenon manifests bactericidal activity in IONPs through oxidative stress which blocks the synthesis of proteins and causes a restriction in further growth of the organism. The bactericidal efficiency of IONPs increased with an increase in concentration and acts as a dose-dependent medicine. Therefore, the inhibited growth of the bacterial species is the reflection of damage and destruction to the cell membrane and is indicative of antimicrobial activity and cell destruction activity induced by nanomaterials that penetrate the cytoplasmic membrane (10).

The MIC of synthesized and characterized Fe_3O_4NPwere determined using the bacteria-ferrous oxide NPs for seven gram-positive and negative bacterial isolates and significant antibacterial effects were estimated on all strains, compared with untreated control. Eventually, this complex could significantly inhibit gram-negative more than gram-positive bacteria.

Authors' Contribution

Study concept and design: M. A.
Acquisition of data: N. H. A. L. A.
Analysis and interpretation of data:
Drafting of the manuscript: A. A. T.
Critical revision of the manuscript for important intellectual content: M. A.
Statistical analysis: M. A.
Administrative, technical, and material support: N. H. A. L. A. and M. A.

Ethics

All the procedures were approved by the Ethics Committee at the Al-Iraqia University, Baghdad, Iraq. Under the project number of 2021-78745-7894.

Conflict of Interest

The authors declare that they have no conflict of interest.

Grant Support

The authors received no specific grant from funding agencies in the public, commercial, or not-for-profit sectors.

Acknowledgment

The authors would like to thank the staff of Al Iraqia College of Medicine, Department of Microbiology for their assistance and support.

References

1. Abrams P, Cardozo L, Fall M, Griffiths D, Rosier P, Ulmsten U, et al. The standardisation of terminology in lower urinary tract function: report from the standardisation sub-committee of the International Continence Society. Urology. 2003;61(1):37-49.
2. Tektook NK, Al-Lehibi KI, Al-Husseinei RK. Prevalence some pathogenic bacteria causing uti in diabetic patients in/specialized center for endocrinology and diabetes of baghdad city–iraq. Med J Babylon. 2017;14(2):260-6.
3. Cotter M, Donlon S, Roche F, Byrne H, Fitzpatrick F. Healthcare-associated infection in Irish long-term care

facilities: results from the First National Prevalence Study. J Hosp Infect. 2012;80(3):212-6.
4. Curns AT, Holman RC, Sejvar JJ, Owings MF, Schonberger LB. Infectious disease hospitalizations among older adults in the United States from 1990 through 2002. Arch Intern Med. 2005;165(21):2514-20.
5. Aljanaby AAJ, Medhat AR. Research article prevalence of some antimicrobials resistance associated-genes in Salmonella typhi isolated from patients infected with typhoid fever. J Biol Sci. 2017;17(4):171-84.
6. Naderi A, Kasra-Kermanshahi R, Gharavi S, Fooladi AAI, Alitappeh MA, Saffarian P. Study of antagonistic effects of Lactobacillus strains as probiotics on multi drug resistant (MDR) bacteria isolated from urinary tract infections (UTIs). Iran J Basic Med Sci. 2014;17(3):201.
7. Nigussie D, Amsalu A. Prevalence of uropathogen and their antibiotic resistance pattern among diabetic patients. Turk J Urol. 2017;43(1):85.
8. Bakhshi B, Dehghan-Mouriaabadi A, Kiani P. Heterogeneity of multidrug-resistant Salmonella enterica isolates with increasing frequency of resistance to Ciprofloxacin during a 4-year period in Iran. Microb Drug Resist. 2018;24(4):479-88.
9. Das R, Perrelli E, Towle V, Van Ness PH, Juthani-Mehta M. Antimicrobial susceptibility of bacteria isolated from urine samples obtained from nursing home residents. Infect Control Hosp Epidemiol. 2009;30(11):1116-9.
10. Das S, Diyali S, Vinothini G, Perumalsamy B, Balakrishnan G, Ramasamy T, et al. Synthesis, morphological analysis, antibacterial activity of iron oxide nanoparticles and the cytotoxic effect on lung cancer cell line. Heliyon. 2020;6(9):e04953.
11. Ismail RA, Sulaiman GM, Abdulrahman SA, Marzoog TR. Antibacterial activity of magnetic iron oxide nanoparticles synthesized by laser ablation in liquid. Mater Sci Eng C. 2015;53:286-97.
12. Khatami M, Aflatoonian MR, Azizi H, Mosazade F, Hoshmand A, Nobre MAL, et al. Evaluation of antibacterial activity of iron oxide nanoparticles against Escherichia coli. practice. 2017;18:19.
13. Khatami M, Alijani H, Sharifi I, Sharifi F, Pourseyedi S, Kharazi S, et al. Leishmanicidal activity of biogenic Fe_3O_4 nanoparticles. Sci Pharm. 2017;85(4):36.
14. Cohen ML. Changing patterns of infectious disease. Nature. 2000;406(6797):762-7.
15. Huang Z, Zheng X, Yan D, Yin G, Liao X, Kang Y, et al. Toxicological effect of ZnO nanoparticles based on bacteria. Langmuir. 2008;24(8):4140-4.
16. Masadeh MM, Karasneh GA, Al-Akhras MA, Albiss BA, Aljarah KM, Al-Azzam SI, et al. Cerium oxide and iron oxide nanoparticles abolish the antibacterial activity of ciprofloxacin against gram positive and gram negative biofilm bacteria. Cytotechnology. 2015;67(3):427-35.
17. M Tille P. Bailey & Scott's Diagnostic Microbiology Fourteenth Edition. Elsevier; 2017.
18. Al-Mudallal N. H. A. L., Khudair A. M., AlsakiniA.l H. , N.A. Z. Molecular detection and Phylogenetic analysis of 16s RNA gene of Proteus mirabilis isolated from different clinical sources in Baghdad hospitals. 2021.
19. Alzahrani E. Gum Arabic-coated magnetic nanoparticles for methylene blue removal. Int J Innov Res Sci Eng Technol. 2014;3(8):15118-29.
20. Khashan KS, Jabir MS, Abdulameer FA. Carbon Nanoparticles decorated with cupric oxide Nanoparticles prepared by laser ablation in liquid as an antibacterial therapeutic agent. Materials Research Express. 2018;5(3):035003.
21. Rashed MM, Al-Mudallal NH, Taha AA. Reduce the toxicity of prepared copper sulfide nanoparticles. Int J Pharm Sci. 2019;10(3):2099-103.
22. Pua F-L, Chia CH, Zakari S, Liew TK, Yarmo MA, Huang NM. Preparation of transition metal sulfide nanoparticles via hydrothermal route. Sains Malays. 2010;39(2):243-8.
23. Daniel WW, Cross CL. Biostatistics: a foundation for analysis in the health sciences: Wiley; 2018.
24. Wayne W, Daniel D, Chad L. Biostatistics. Basic concepts and methodology for the health sciences. New Delhi:. 2010.
25. Nicolle LE, Bradley S, Colgan R, Rice JC, Schaeffer A, Hooton TM. Infectious Diseases Society of America guidelines for the diagnosis and treatment of asymptomatic bacteriuria in adults. Clin Infect Dis. 2005:643-54.
26. Nicolle LE, Committee SL-TC. Urinary tract infections in long-term–care facilities. nfect Control Hosp Epidemiol. 2001;22(3):167-75.
27. High KP, Juthani-Mehta M, Quagliarello VJ. Infectious diseases in the nursing home setting: challenges and opportunities for clinical investigation. Clin Infect Dis. 2010;51(8):931-6.

28. Abdulrahman IS. Antimicrobial scesuptibility pattern of pathogenic bacteria causing urinary tract infection at Azadi hospital in Duhok city, Kurdistan region, Iraq. Sci J Univ Zakho. 2018;6(2):46-50.
29. Yassin NA. Laboratory evaluation of urine culture and drug resistance in outpatients clincally suspected of urinary tract infections. Rawal Medical J. 2012;37:268-72.
30. Hasany S, Ahmed I, Rajan J, Rehman A. Systematic review of the preparation techniques of iron oxide magnetic nanoparticles. Nanosci Nanotechnol. 2012;2(6):148-58.
31. Huber DL. Synthesis, properties, and applications of iron nanoparticles. Small. 2005;1(5):482-501.
32. Amendola V, Riello P, Meneghetti M. Magnetic nanoparticles of iron carbide, iron oxide, iron@ iron oxide, and metal iron synthesized by laser ablation in organic solvents. J Phys Chem C. 2011;115(12):5140-6.
33. Estelrich J, Escribano E, Queralt J, Busquets MA. Iron oxide nanoparticles for magnetically-guided and magnetically-responsive drug delivery. Int J Mol Sci. 2015;16(4):8070-101.
34. Mohapatra M, Anand S. Synthesis and applications of nano-structured iron oxides/hydroxides–a review. Int J Eng Sci Technol. 2010;2(8).
35. Hyeon T. Chemical synthesis of magnetic nanoparticles. Chem Commun. 2003(8):927-34.
36. Xu J, Sun J, Wang Y, Sheng J, Wang F, Sun M. Application of iron magnetic nanoparticles in protein immobilization. Molecules. 2014;19(8):11465-86.
37. Bao S, Li K, Ning P, Peng J, Jin X, Tang L. Highly effective removal of mercury and lead ions from wastewater by mercaptoamine-functionalised silica-coated magnetic nano-adsorbents: behaviours and mechanisms. Appl Surf Sci. 2017;393:457-66.
38. Armijo LM, Wawrzyniec SJ, Kopciuch M, Brandt YI, Rivera AC, Withers NJ, et al. Antibacterial activity of iron oxide, iron nitride, and tobramycin conjugated nanoparticles against Pseudomonas aeruginosa biofilms. J Nanobiotechnology. 2020;18(1):1-27.
39. Li F, Liang Z, Liu J, Sun J, Hu X, Zhao M, et al. Dynamically reversible iron oxide nanoparticle assemblies for targeted amplification of T1-weighted magnetic resonance imaging of tumors. Nano Lett. 2019;19(7):4213-20.
40. Madhu G, Jaianand K, Rameshkumar K, Eyini M, Balaji P, Veeramanikandan V. Solanum tuberosum extract mediated synthesis and characterization of iron oxide nanoparticles for their antibacterial and antioxidant activity. J Drug Deliv Sci Technol. 2019;9(1-s):5-15.
41. Prodan AM, Iconaru SL, Chifiriuc CM, Bleotu C, Ciobanu CS, Motelica-Heino M, et al. Magnetic properties and biological activity evaluation of iron oxide nanoparticles. J Nanomater. 2013;2013.
42. Taylor E, Webster TJ. Reducing infections through nanotechnology and nanoparticles. Int J Nanomedicine. 2011;6:1463.
43. Gordon T, Perlstein B, Houbara O, Felner I, Banin E, Margel S. Synthesis and characterization of zinc/iron oxide composite nanoparticles and their antibacterial properties. Colloid Surf A-Physicochem Eng Asp 2011;374(1-3):1-8.
44. Van Acker H, Gielis J, Acke M, Cools F, Cos P, Coenye T. The role of reactive oxygen species in antibiotic-induced cell death in Burkholderia cepacia complex bacteria. PloS one. 2016;11(7):e0159837.